MRS Advances (2022) 7:736–740
https://doi.org/10.1557/s43580-022-00344-w

ORIGINAL PAPER

Microstructure and dielectric properties of $CaCu_3Ti_4O_{12}$ ceramics by lanthanum/europium co-doping

Yong Guo[1] · Junlang Tan[1] · Jingchang Zhao[1]

Received: 28 June 2022 / Accepted: 31 August 2022 / Published online: 12 September 2022

Abstract

In this work, (La, Eu) co-doped $CaCu_3Ti_4O_{12}$ ceramics ($Ca_{1-x}La_xCu_3Ti_{4-x}Eu_xO_{12}$(CLCTEO)), $x = 0.1$, 0.3, and 0.5) were prepared by the solid-state method. The phase structure, morphologies, dielectric properties, and impedance spectrum were investigated methodically. The XRD of CLCTEO ceramics confirmed the formation of the complex perovskite with a residual amount of $CaTiO_3$. The refined calculation found that the lattice parameter of CLCTEO ceramics will significantly increase due to the co-doping of La and Eu. The FESEM analysis shows that the grain size of co-doped CCTO is smaller, reaching the nanometer scale. Impedance indicates that the (La, Eu) co-doped CCTO ceramics have higher dielectric permittivity than the single-doped with La or Eu. The results show that co-doping is an effective method to improve the dielectric properties of CCTO ceramics.

Introduction

Due to the importance of miniaturizing the electronic components in microelectronic devices, materials with giant dielectric permittivity (ε_r) have attracted significant attention for their potential application in supercapacitor, varistors, and resonators [1, 2]. The perovskite-like oxide $CaCu_3Ti_4O_{12}$ (CCTO) exhibited relatively high dielectric permittivity (10^4–10^5) in the wide frequency range of 10^2–10^6 Hz and good temperature stability in a specific temperature range (100–600 K) [3, 4]. Furthermore, CCTO is a lead-free material with non-linear current–voltage property [5]. Such properties make CCTO promising candidates for use in microelectronic applications [6, 7].

However, the large dielectric loss (tanδ) of CCTO limits its further practical applications in device development [8, 9]. Besides, the mechanism originating from CCTO of high performance remains controversial [10, 11]. Several models, such as internal barrier layer capacitance (IBLC), surface barrier layer capacitor (SBLC), and interface polarization, are used to interpret its dielectric behavior [12–15]. Among these, the IBLC model composed of semi-conducting grains and insulating grain boundaries is widely accepted by most scholars. However, this model is unsuitable for explaining the dielectric behavior of single crystals.

Meanwhile, many methods were applied to improve the dielectric properties of CCTO. Liu et al. reported that Eu-doped CCTO ceramics have a sharp decrease in both the ε_r and electric resistance of the grain boundary [16]. Cheng et al. discovered that La-doped CCTO ceramics could maintain the high ε_r at room temperature [17]. Salam et al. claimed that (Sr, Ni) co-doped CCTO ceramics have better dielectric properties than Sr-doped CCTO and Ni-doped CCTO ceramics [18]. Similar co-doping also achieved good performance compared with single-element doping, such as (La, Zn) [19], (Sr, La) [4], (Li, Al)[20], (Nb, Zr) [21], (Sr, F) [22], (Y, Zn) [23], (Zn, Al) [24]. Nevertheless, there are a few reports on the dielectric properties of La and Eu co-doped CCTO ceramics. In this paper, $Ca_{1-x}La_xCu_3Ti_{4-x}Eu_xO_{12}$ ceramics (CLCTEO, $x = 0.1$, 0.3, and 0.5) were fabricated by the solid-state method.

Experimental and characterization

The La and Eu co-doped $CaCu_3Ti_4O_{12}$ ceramics with the formula $Ca_{1-x}La_xCu_3Ti_{4-x}Eu_xO_{12}$ ($x = 0.1$, 0.3, and 0.5) were synthesized by the traditional solid-state method. The analytical grade calcium carbonate ($CaCO_3$, 99.9%, Aladdin), cupric oxide (CuO, 99.9%, Aladdin), titanium dioxide (TiO_2, 99.9%, Aladdin), lanthanum oxide (La_2O_3, 99.9%,

✉ Jingchang Zhao
jchzhao@ynu.edu.cn

[1] Present Address: School of Materials and Energy, Yunnan University, Kunming 650091, People's Republic of China

Aladdin), and europium trioxide (Eu_2O_3, 99.9%, Aladdin) were weighed according to the stoichiometric formula and milled with zirconium balls at 300 rpm for 36 h in ethanol medium. The mixtures were then dried in an oven for 8 h and calcinated at 920 °C in air atmosphere for 8 h. The powders were thoroughly ground with an agate mortar and pressed into green pellets (diameter 8 mm, thickness 1.2 mm) under a pressure of 30 MPa. The green pellets were sintered in air at 1040 °C for 6 h to obtain the dense ceramics.

The phase composition and crystal structure of these ceramics were obtained at R.T. by us an X-ray diffraction meter (XRD, D8 ADVANCE DaVinci, Germany) with CuKα radiation under the conditions of 40 kV and 30 mA. The surface microstructural features of the ceramics were studied using a field emission scanning electron microscope (FMSEM, Nano SEM 450, Germany). The valence states of elements were examined using X-ray photoelectron spectroscopy (XPS, K-Alpha+, USA). For electrical performance measurements, the ceramics were polished and then coated with silver electrodes for 5 min at 12 mA using an ETD 3000 sputter coating unit. The dielectric properties and impedance spectroscopy were measured by Agilent 4284A Precision Impedance Analyzer in the frequency range of 20 Hz to 1 MHz.

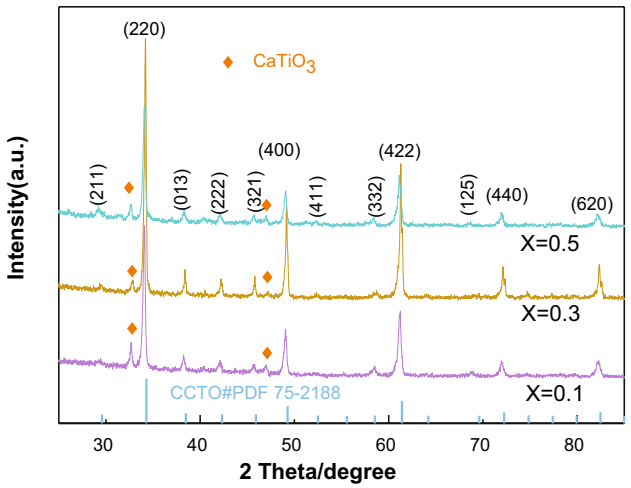

Fig. 1 XRD patterns of $Ca_{1-x}La_xCu_3Ti_{4-x}Eu_xO_{12}$ ceramics ($x=0.1$, 0.3, and 0.5)

Results and discussion

The XRD patterns of $Ca_{1-x}La_xCu_3Ti_{4-x}Eu_xO_{12}$ ceramics ($x=0.1$, 0.3, and 0.5) are shown in Fig. 1. The diffraction peaks for the (220), (013), (222), (400), (422), and (620) crystal planes of all samples completely match the CCTO standard card (JCPDS-75–2188), indicating the polycrystalline complex perovskite phases were successfully synthesized. Besides, a small amount of $CaTiO_3$ also appears in all samples, which may be caused by the substitution of La and Eu for Ca and Ti. Similar phenomena have also been reported in (Sr, La) co-doped CCTO [4]. This refined calculation found that the lattice parameters of $Ca_{1-x}La_xCu_3Ti_{4-x}Eu_xO_{12}$ ceramics ($x=0.1$, 0.3, and 0.5) are 7.4048, 7.4234 and 7.441, respectively. Compared with pure CCTO, the increase in the value of lattice parameter is mainly attributed to the larger ionic radius of the La^{3+} (115 pm) compared to the Ca^{2+} (105 pm) and Eu^{3+} (94.7 pm) compared to the Ti^{3+} (60.5 pm). Similar results have also been reported in the literature [25].

The FESEM micrograph of $Ca_{1-x}La_xCu_3Ti_{4-x}Eu_xO_{12}$ ceramics ($x=0.1$, 0.3, and 0.5) are shown in Fig. 2. Ceramics with prominent crystal characteristics and dense microstructure were obtained by sintering at 1040 °C for 6 h. It also can be observed that ceramics are composed of particles with the particle sizes from nm to a few μm, and their morphology and structure are greatly affected by (La, Eu) co-doping. Simultaneously, the results show that as the concentration of co-doped (La, Eu) ions increases, the grain size decreases slightly. The above results indicate that grain growth can be suppressed by co-doping (La, Eu). Similar effects of co-doping in CCTO have been reported by Rodrigo et al. in co-doping (Sr, La) [26] and Pu et al. in co-doping (Zr, Nb) [11].

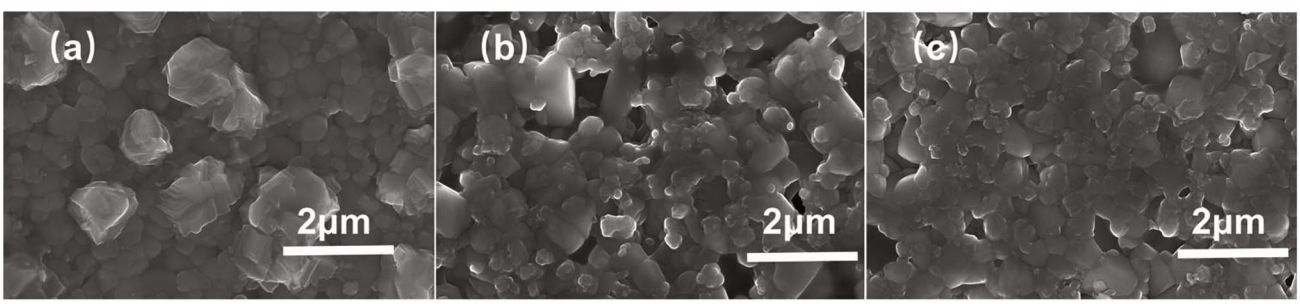

Fig. 2 FESEM micrograph of surfaces of $Ca_{1-x}La_xCu_3Ti_{4-x}Eu_xO_{12}$ ceramics, (a) $x=0.1$, (b) $x=0.3$, and (c) $x=0.5$

The frequency dependence of ε_r (a) and tanδ (b) of the $Ca_{1-x}La_xCu_3Ti_{4-x}Eu_xO_{12}$ ceramics ($x=0.1$, 0.3, and 0.5) at room temperature are given in Fig. 3. As shown in Fig. 3(a), the ε_r value of all ceramics maintains the high dielectric properties (10^4) in the range from 20 Hz to 4 kHz. For instance, at frequency $f=100$ Hz, ε_r is about 9.6×10^4, 1.4×10^5, 8.2×10^4, respectively. Compared to Eu or La single-doped CCTO ceramics, it can be found that CLCTEO ceramics has better dielectric properties [27]. The value of ε_r for the CLCTEO ceramics is relatively stable and nearly independent of the range from 10 kHz to 1 MHz. It was reported that the large ε_r-value at low frequency may be related to the interface polarization of the electrode contact [15]. The CLCTEO ceramics showed a Debye-type relaxation behavior originating from the interfacial polarization between the crystal grains and grain boundaries [28]. As shown in Fig. 3(b), the tanδ of CLCTEO ceramics increases with increasing (La, Eu) concentration x within the whole frequency range of measurement. For the CLCTEO ceramics with $x=0.3$ and 0.5, their tanδ values are quite close, even though the former is slightly smaller than the latter. The minimum tanδ for CLCTEO ceramics is only 0.013 at 800 kHz when $x=0.1$.

The XPS spectrum of $Ca_{1-x}La_xCu_3Ti_{4-x}Eu_xO_{12}$ with $x=0.3$ is shown in Fig. 3, where (c) is the full spectrum, (d) and (e) are the fine spectra of La and Eu, respectively. The prominent element peaks such as C 1s, O 1s, Ca 2p, Ti 2p, Cu 2p, La 3d5, and Eu 3d5 can be observed in the full spectrum of $Ca_{1-x}La_xCu_3Ti_{4-x}Eu_xO_{12}$ with $x=0.3$, where C 1s is the corrective element. A fine spectrum scan was deliberately carried out to study further the chemical state of the doped elements La and Eu. In Fig. 3(d), it can be observed that the two peaks of La $3d_{5/2}$ are located at 833.59 eV and 837.95 eV, respectively. The bond energy difference between the two peaks is 4.36 eV, close to the 4.6 eV of the complex La_2O_3, indicating the successful doping of La. Moreover, it can be found that the bond energy of the Eu $3d_{5/2}$ peak is 1133.60 eV in Fig. 3(e), which is close to the 1134.8 eV of Eu^{3+} reported in the literature [29], and there is also a shake-down satellite peak, which proves that Eu^{3+} comes from Eu_2O_3.

The complex impedance spectra of $Ca_{1-x}La_xCu_3Ti_{4-x}Eu_xO_{12}$ ceramics ($x=0.1$, 0.3, and 0.5) measured at RT are displayed in Fig. 4. For all samples, two semicircular arcs can be observed in the whole frequency range. The grain resistance and grain boundary resistance are represented by a large arc and a small arc [30]. The measurement results of complex impedance spectroscopy indicated that the response could be modeled by an IBLC equivalent circuit, as shown in Fig. 4. Therefore, the equivalent circuit can be made up of two parallel R.C. elements in series. The grain resistance, grain boundary resistance, and constant phase angle element are represented by R_g, R_{gb}, and CPE. According to the model, the decrease in grain boundary resistance and the substantial increase in grain boundary resistance cause polarization loss. It can be found that the doping of La and

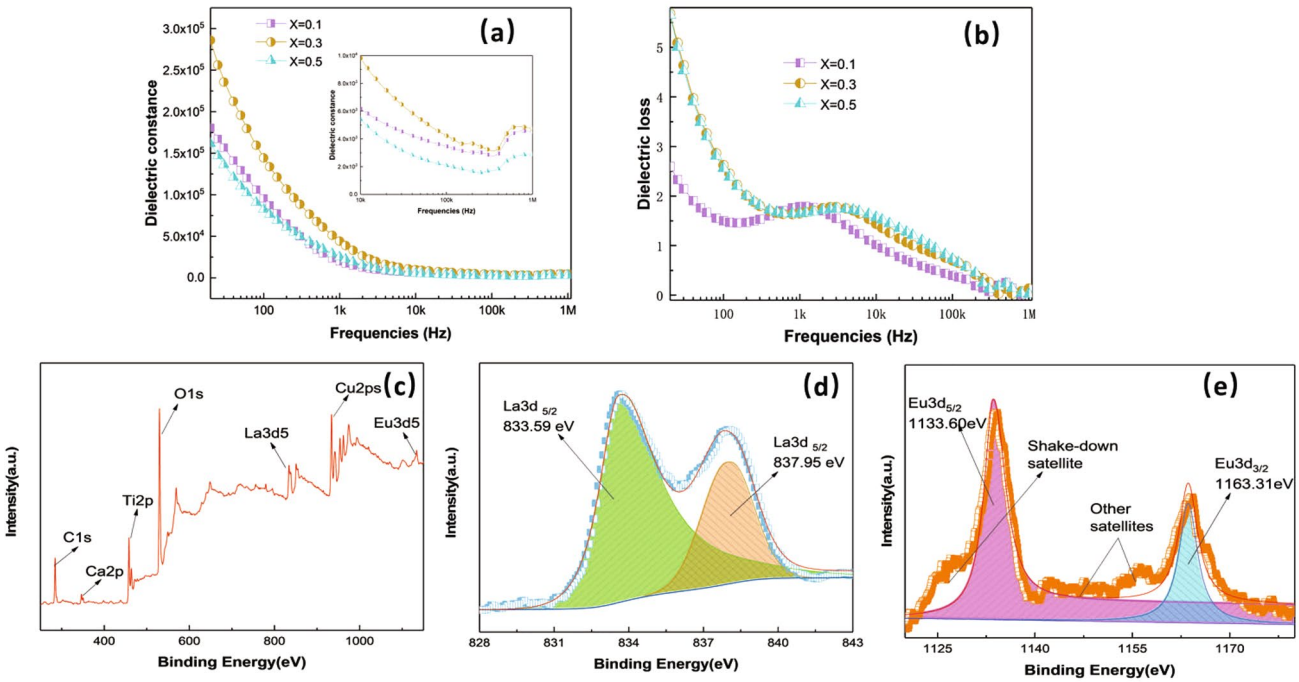

Fig. 3 Dielectric properties and XPS spectra of $Ca_{1-x}La_xCu_3Ti_{4-x}Eu_xO_{12}$ ceramics ($x=0.1$, 0.3, and 0.5), (a) dielectric constant, (b) dielectric loss, (c) full spectrum of XPS, (d) and (e) are the fine spectra of La and Eu, respectively

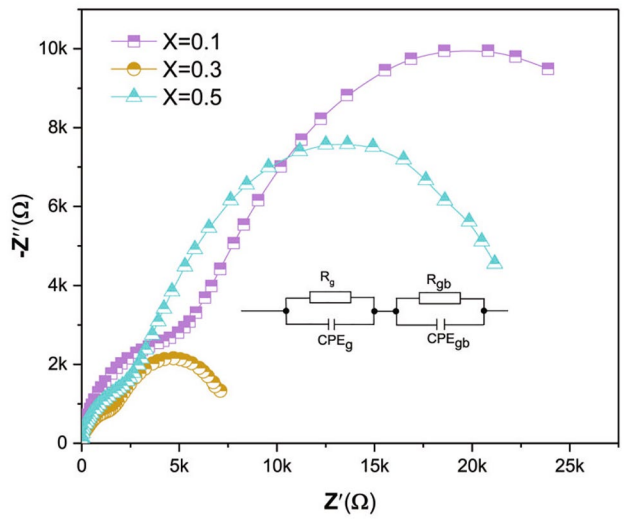

Fig. 4 Complex impedance spectra of $Ca_{1-x}La_xCu_3Ti_{4-x}Eu_xO_{12}$ ceramics ($x=0.1$, 0.3, and 0.5). The inset shows the corresponding equivalent circuit model

Eu has a significant influence on the R_g and R_{gb}, especially on the R_{gb}. It can be observed that the R_{gb} decreases with the increase of (La, Eu) co-doping concentration, which is consistent with the dielectric loss value displayed in Fig. 3(b). The dielectric loss decreases with the increase of grain boundary resistance. Based on the above results, the dielectric properties of CLCTEO ceramics may be derived from the interfacial polarization of the grain boundaries.

Conclusion

(La, Eu) co-doped CCTO ceramics were successfully prepared using a solid-state synthesis method. The results show that the concentration of doped ions greatly influences the microstructure and dielectric properties of the materials. The lattice parameter increased with the increase of doping concentration since the ion radius of La and Eu is larger than that of Ca and Cu. The FESEM image indicates that the morphology of CLCTEO ceramics was distinctly affected by La and Eu doping. The XPS proves that La and Eu in CLCTEO lattices are derived from La_2O_3 and Eu_2O_3 dopants, respectively. The dielectric constant of (La, Eu) co-doped $Ca_{1-x}La_xCu_3Ti_{4-x}Eu_xO_{12}$ ceramics reached a higher value than that of La or Eu single-doped CCTO ceramics. Obviously, (La, Eu) co-doped can effectively improve the dielectric properties of CCTO ceramics.

Acknowledgments This work was supported by the Natural Science Foundation of China (51562037) and Yunnan University Graduate Research and Innovation Fund (2020Z41). The authors thank the Advanced Analysis and Measurement Center of Yunnan University for the sample testing service.

Author contributions JZ: Conceptualization, Methodology, Software, Funding acquisition; YG: Data curation, Writing-Original draft preparation, Visualization, Investigation, Writing-Reviewing and Editing; JT: Supervision, Software, Validation.

Data availability The datasets generated and analyzed during the current study are available from the corresponding author on reasonable request.

Declarations

Conflict of interest There are no conflicts of interest to declare.

References

1. J. Zhao, H. Zhao, Z. Zhu, Influence of sintering conditions and CuO loss on dielectric properties of $CaCu_3Ti_4O_{12}$ ceramics. Mater. Res. Bull. **113**, 97 (2019)
2. M.S. Ivanov, F. Amaral, V.A. Khomchenko, L.C. Costa, J.A. Paixao, A novel approach to study the conductivity behavior of $CaCu_3Ti_4O_{12}$ using scanning probe microscopy technique. MRS Commun. **8**, 932 (2018)
3. S. Pongpaiboonkul, T.M. Daniels, J.H. Hodak, A. Wisitsoraat, S.K. Hodak, Preferentially oriented Fe-doped $CaCu_3Ti_4O_{12}$ films with high dielectric constant and low dielectric loss deposited on $LaAlO_3$ and $NdGaO_3$ substrates. Appl. Surf. Sci. **540**(1), 148373 (2021)
4. R. Espinoza-González, S. Hevia, Á. Adrian, Effects of strontium/lanthanum co-doping on the dielectric properties of $CaCu_3Ti_4O_{12}$ prepared by reactive sintering. Ceram. Int. **44**, 15588 (2018)
5. D.S. Saidina, A. Norshamira, M. Mariatti, Dielectric and thermal properties of CCTO/epoxy composites for embedded capacitor applications: mixing and fabrication methods. J. Mater. Sci. Mater. Electron. **26**, 8118 (2015)
6. E.C. Grzebielucka, J.F.H. Leandro Monteiro, E.C.F. de Souza, C.P. Ferreira Borges, A.V.C. de Andrade, E. Cordoncillo, H. Beltrán-Mir, S.R.M. Antunes, Improvement in varistor properties of $CaCu_3Ti_4O_{12}$ ceramics by chromium addition. J. Mater. Sci. Technol. **41**, 12 (2020)
7. Y. Qing, Z. Yang, Q. Wen, F. Luo, $CaCu_3Ti_4O_{12}$ particles and MWCNT-filled microwave absorber with improved microwave absorption by FSS incorporation. Appl. Phys. A **122**, 640 (2016)
8. T.-T. Fang, L.-T. Mei, Evidence of Cu deficiency: a key point for the understanding of the mystery of the giant dielectric constant in $CaCu_3Ti_4O_{12}$. J. Am. Ceram. Soc. **90**, 638 (2007)
9. Y. Guo, J. Tan, J. Zhao, Microstructure and electrical properties of nano-scale SnO_2 hydrothermally coated CCTO-based composite ceramics. Ceram. Int. **48**(12), 17795–17801 (2022)
10. Y. Zhu, T. Wang, W. Wang, S. Chen, E. Lichtfouse, C. Cheng, J. Zhao, Y. Li, C. Wang, $CaCu_3Ti_4O_{12}$, an efficient catalyst for ibuprofen removal by activation of peroxymonosulfate under visible-light irradiation. Environ. Chem. Lett. **17**, 481 (2018)
11. P. Mao, J. Wang, P. Xiao, L. Zhang, F. Kang, H. Gong, Colossal dielectric response and relaxation behavior in novel system of Zr^{4+} and Nb^{5+} co-substituted $CaCu_3Ti_4O_{12}$ ceramics. Ceram. Int. **47**, 111 (2021)
12. D.C. Sinclair, T.B. Adams, F.D. Morrison, A.R. West, $CaCu_3Ti_4O_{12}$: one-step internal barrier layer capacitor. Appl. Phys. Lett. **80**, 2153 (2002)

13. H. Lin, W. Xu, H. Zhang, C. Chen, Y. Zhou, Z. Yi, Origin of high dielectric performance in fine grain-sized $CaCu_3Ti_4O_{12}$ materials. J. Eur. Ceram. Soc. **40**, 1957 (2020)
14. S.F. Shao, J.L. Zhang, P. Zheng, W.L. Zhong, C.L. Wang, Microstructure and electrical properties of $CaCu_3Ti_4O_{12}$ ceramics. J. Appl. Phys. (2006). https://doi.org/10.1063/1.2191447
15. B.S. Prakash, K.B.R. Varma, Influence of sintering conditions and doping on the dielectric relaxation originating from the surface layer effects in $CaCu_3Ti_4O_{12}$ ceramics. J. Phys. Chem. Solids **68**, 490 (2007)
16. J.-W. Liu, D.-Y. Lu, X.-Y. Yu, Q.-L. Liu, Q. Tao, H. Change, P.-W. Zhu, Dielectric properties of Eu-doped $CaCu_3Ti_4O_{12}$ with different compensation mechanisms. Acta Metall. Sin. (Engl. Lett.) **30**, 97 (2016)
17. B. Cheng, Y.-H. Lin, J. Yuan, J. Cai, C.-W. Nan, X. Xiao, J. He, Dielectric and nonlinear electrical behaviors of La-doped $CaCu_3Ti_4O_{12}$ ceramics. J. Appl. Phys. (2009). https://doi.org/10.1063/1.3194311
18. S. Rhouma, S. Saîd, C. Autret, S. De Almeida-Didry, M. El Amrani, A. Megriche, Comparative studies of pure, Sr-doped, Ni-doped and co-doped $CaCu_3Ti_4O_{12}$ ceramics: enhancement of dielectric properties. J. Alloys Compd. **717**, 121 (2017)
19. S. Rani, N. Ahlawat, R. Punia, K.M. Sangwan, P. Khandelwal, Dielectric and impedance studies of La and Zn co-doped complex perovskite $CaCu_3Ti_4O_{12}$ ceramic. Ceram. Int. **44**, 23125 (2018)
20. L. Sun, Q. Ni, J. Guo, E. Cao, W. Hao, Y. Zhang, L. Ju, Dielectric properties and nonlinear I–V electrical behavior of (Li^{1+}, Al^{3+}) co-doped $CaCu_3Ti_4O_{12}$ ceramics. Appl. Phys. A **124**, 428 (2018)
21. S. Rani, N. Ahlawat, K.M. Sangwan, S. Rani, R. Punia, J. Malik, Structural investigation and giant dielectric response of $CaCu_3Ti_4O_{12}$ ceramic by Nd/Zr co-doping for energy storage applications. J. Mater. Sci. Mater. Electron. **29**, 10825 (2018)
22. J. Jumpatam, B. Putasaeng, N. Chanlek, J. Boonlakhorn, P. Thongbai, N. Phromviyo, P. Chindaprasirt, Significantly improving the giant dielectric properties of $CaCu_3Ti_4O_{12}$ ceramics by co-doping with Sr^{2+} and F^- ions. Mater. Res. Bull. (2021). https://doi.org/10.1016/j.materresbull.2020.111043
23. J. Boonlakhorn, P. Kidkhunthod, N. Chanlek, P. Thongbai, Effects of DC bias on dielectric and electrical responses in (Y + Zn) co-doped $CaCu_3Ti_4O_{12}$ perovskite oxides. J. Mater. Sci. Mater. Electron. **28**, 4695 (2016)
24. C. Xu, X. Zhao, L. Ren, J. Sun, L. Yang, J. Guo, R. Liao, Enhanced electrical properties of $CaCu_3Ti_4O_{12}$ ceramics by spark plasma sintering: role of Zn and Al co-doping. J. Alloys Compd. **792**, 1079 (2019)
25. M. Xiao, P. Sheng, Nonlinear current–voltage behavior in La-doped $CaCu_3Ti_4O_{12}$ thin films derived from sol–gel method. J. Mater. Sci. Mater. Electron. **27**, 9483 (2016)
26. A.A. Felix, M. Spreitzer, D. Vengust, D. Suvorov, M.O. Orlandi, Probing the effects of oxygen-related defects on the optical and luminescence properties in $CaCu_3Ti_4O_{12}$ ceramics. J. Eur. Ceram. Soc. **38**, 5002 (2018)
27. S. Jin, H. Xia, Y. Zhang, Effect of La-doping on the properties of $CaCu_3Ti_4O_{12}$ dielectric ceramics. Ceram. Int. **35**, 309 (2009)
28. C. Mu, H. Zhang, Y. He, P. Liu, Influence of temperature on dielectric properties of Fe-doped $CaCu_3Ti_4O_{12}$ ceramics. Physica B **405**, 386 (2010)
29. F. Mercier, C. Alliot, L. Bion, N. Thromat, P. Toulhoat, XPS study of Eu(III) coordination compounds: core levels binding energies in solid mixed-oxo-compounds EumXxOy. J. Electron Spectrosc. Relat. Phenom. **150**, 21 (2006)
30. R. Schmidt, M.C. Stennett, N.C. Hyatt, J. Pokorny, J. Prado-Gonjal, M. Li, D.C. Sinclair, Effects of sintering temperature on the internal barrier layer capacitor (IBLC) structure in $CaCu_3Ti_4O_{12}$ (CCTO) ceramics. J. Eur. Ceram. Soc. **32**, 3313 (2012)